Exchange Effects in an Artificial Atom at High Magnetic Fields

O. Klein, C. de C. Chamon, D. Tang, D. M. Abusch-Magder, U. Meirav,* X.-G. Wen, and M. A. Kastner
Physics Department, Massachusetts Institute of Technology, 77 Massachusetts Avenue, Cambridge, Massachusetts 02139

S. J. Wind
IBM T.J. Watson Research Center, Yorktown Heights, New York 10598
(Received 7 July 1994)

A droplet of $N \sim 30$ electrons is created by lateral confinement of a two-dimensional electron gas. The evolution of its chemical potential μ_N with magnetic field B is inferred from resonant tunneling experiments and is used to study the dependence of its magnetization on B. The experimental data, quantitatively described by Hartree-Fock theory, suggest a divergent spin susceptibility at B_c implying a ground state of minimum total spin just below B_c. In the spin polarized regime we observe a new phase also predicted by Hartree-Fock theory.

PACS numbers: 73.20.Dx, 73.20.Mf

Recent experiments [1,2] have demonstrated the possibility of measuring the chemical potential μ_N of a droplet of N electrons created by lateral confinement of a two-dimensional electron gas; such confined systems can be thought of as artificial atoms [3]. Abrupt shifts of μ_N occur at values of the magnetic field B at which the ground state (GS) of the droplet changes. These results have stimulated calculations [4–10] of the B-N phase diagram, in which each phase is designated by the quantum numbers of the GS; the shifts in $\mu_N(B)$ happen at the phase boundaries. In particular, MacDonald, Yang, and Johnson [9] and Chamon and Wen [10] have independently predicted new phases of a spin polarized droplet in a parabolic potential at high B. These phases are especially interesting because any transition in the spin polarized regime is a consequence of many-body phenomena that cannot be explained by a single-electron picture.

In this Letter, we present measurements of a portion of the B-N phase diagram, and we use a new approach for comparing the experimental results with theoretical models. We find that Hartree-Fock (HF) [9,10] theory provides a quantitative description when both spin states of the lowest orbital Landau level (LL) are occupied, whereas a semiclassical electrostatic model (SC) [6] does not, indicating that exchange plays an important role. The experimental data indicate a divergent spin susceptibility at B_c confirming a minimum total spin GS predicted by HF just below B_c. We also find evidence for a new phase in the spin polarized regime, which is described qualitatively by HF.

The device that we study is of the type described by Meirav, Kastner, and Wind [11]. It consists of a two-dimensional electron gas (2DEG) in an inverted GaAs/$Al_xGa_{1-x}As$ heterostructure with electrostatic gates above and below it. The bottom gate is a highly conducting substrate of n^+ doped GaAs. A positive bias, V_g, applied to the bottom gate varies the density of the 2DEG. On the top surface of undoped GaAs, two metallic (TiAu) gates are lithographically patterned with a double constriction. Applying a negative bias to these top gates depletes the 2DEG 100 nm underneath them, confining the electrons to an island between the constrictions. Current flows through the resulting electron droplet via the tunnel barriers caused by the constrictions. The top gate geometry of the device under investigation has been examined with an atomic force microscope. We estimate that the region between the constrictions is roughly 500×500 nm^2. According to the simulation of the device by Kumar, Laux, and Stern [12], the external confinement potential of the droplet is approximately parabolic. Although all results presented here are for this one structure, we have observed similar features in samples of different geometries.

The negative bias on the top gate is maintained constant during the experiment and the bottom gate voltage is varied in a narrow range near $V_g = 160 \pm 1$ mV, for which the electron density of the 2DEG regions outside the constrictions is almost constant at $(1.3 \pm 0.01) \times 10^{11}$ cm^2. The conductance G of the device as a function of V_g at $B = 0$ is shown in the lower inset of Fig. 1. It consists of quasiperiodic sharp peaks ($\Delta V_g = 1.2$ mV), crudely described by the Coulomb blockade mechanism [13]. In this model, when the bottom gate voltage is set between peaks, transport is suppressed by the charging energy $U \sim 0.66$ meV necessary to add an electron to the droplet. Each period thus corresponds to the addition of one electron to the droplet. At resonance, the electrochemical potential of the droplet, $\mu_N - e\alpha V_g$, is aligned with the Fermi energy of the leads and current flows; current requires a fluctuation of the charge on the droplet. Thus, the value of V_g at which the peak occurs provides a measure of μ_N. At $T = 0$, $\mu_N = E_N - E_{N-1}$, where E_N is the energy of the N-electron GS.

First, we consider the effect of B on the position of a single conductance peak. That is, we measure $\mu_N(B)$ at constant N. The value of the gate voltage at which the Nth conductance peak occurs is plotted as a function of B between 1 and 5 T in Fig. 1. The change in behavior

0031-9007/95/74(5)/785(4)$06.00

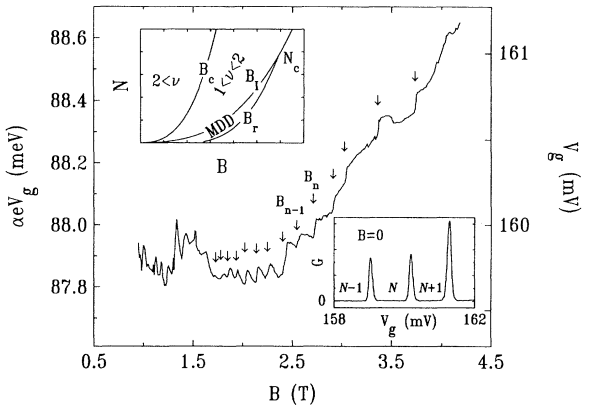

FIG. 1. Upper inset: Theoretical B-N phase diagram of the droplet. The boundaries corresponding to a change of the total spin S in the $2 > \nu > 1$ regime are omitted; the MDD domain of stability is limited on one side by $B_I(N)$, the boundary of the spin polarized phase, and on the other side by $B_r(N)$, where there is the edge reconstruction. Above N_c the MDD phase is terminated. Lower inset: Conductance through the island as a function of the bottom gate voltage at $B = 0$. Main: Position of the Nth conductance peak as a function of B at $T = 100$ mK. We have used a constant factor $\alpha = 0.55$ to convert the bottom gate voltage scale to energy [1,6]. The arrows indicate the minima of the conductance peak height; B_n is the field for the nth minimum above 1.6 T.

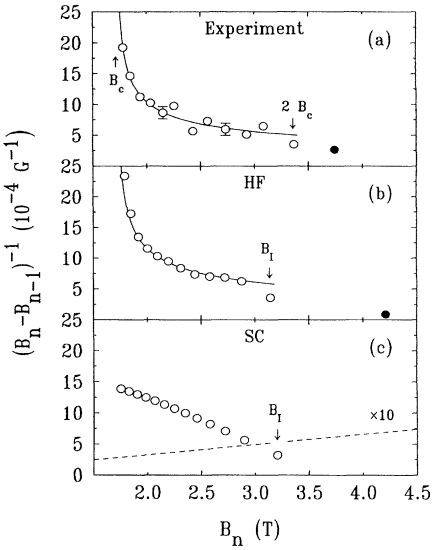

FIG. 2. (a) $(B_n - B_{n-1})^{-1}$ vs the B_n obtained from Fig. 1. The error bars represent the spread of the data when the analysis is repeated for other conductance peaks on the same device. (b),(c) Results obtained with the HF ($N = 27$ and $\hbar\omega_0 = 2.1$ meV) and SC ($N = 42$ and $\hbar\omega_0 = 1.8$ meV) models. The solid lines are fits by $y(B) = y_0[(B - B_c)/B_c]^\epsilon$, where $B_c = 1.7 \pm 0.02$ T and $\epsilon = -0.41 \pm 0.06$ for the experiment and $\epsilon = -0.43 \pm 0.03$ for the HF. The solid circle indicates B_r. The dashed line in (c) is the constant interaction model [6] (the scale is expanded by a factor of 10).

near 1.6 T results from the depopulation of all but the lowest orbital LL [6]. The steplike behavior of the peak position above 1.6 T results from the transfer of electrons between the two spin-split states of the lowest orbital LL [6]. We call $N_\uparrow$ and $N_\downarrow$ the occupations of the lower and upper energy states, respectively. Each step corresponds to a change by one unit of the total spin quantum number $S = (N_\uparrow - N_\downarrow)/2$.

To characterize the data in Fig. 1 we examine the separation in B of the upward steps in μ_N. The peak conductance as a function of B has a sharp minimum at each of these steps [1], which precisely determines B_n, the field for the nth step. (The B_n are indicated by arrows in Fig. 1.) Because each step corresponds to the flip of a spin, one may think of $\chi_n = (B_n - B_{n-1})^{-1}$ as a measure of the spin susceptibility. We plot χ_n as a function of B_n in Fig. 2(a). A fit by the empirical form $y(B) = y_0[(B - B_c)/B_c]^\epsilon$ gives $B_c = 1.7 \pm 0.02$ T and $\epsilon = -0.41 \pm 0.06$ for our data; the solid curve in Fig. 2(a) shows the fit. The same functional form also fits the experimental data for two other devices with different geometries (500×700 and 450×900 nm^2) and larger numbers of steps ($\sim$25 and 35) with $\epsilon = -0.37 \pm 0.1$ for all three devices.

Plotted in Fig. 2(c) is the result obtained when χ_n is determined using μ_N of the SC model [6]. For a parabolic potential with cylindrical symmetry, $V(r) \propto \omega_0^2 r^2$, the SC spatial density of electrons $\rho(r)$ is approximately hemispherical except near r, corresponding to integer filling factors $\nu = 2\pi\ell^2\rho(r)$, where the electrons form an incompressible liquid (ω_0 is the oscillator frequency and ℓ is the magnetic length). At fixed B, $\rho(r)$ is uniquely determined by N and $\hbar\omega_0$. We adjust N so that the calculated $\mu_N(B)$ has the same number of steps as observed experimentally. With N fixed, we adjust $\hbar\omega_0$ to match the value of $B_c = 1.7$ T, at which the transfer of electrons between $N_\downarrow$ and $N_\uparrow$ begins in our experiment. Using this procedure, we find $N = 42$ and $\hbar\omega_0 = 1.8$ meV. As seen in Fig. 2(c), the SC model predicts values of χ_n, which are roughly the same size as the measured ones. However, it does not predict the upward curvature of χ_n near B_c.

To compare our results with a more sophisticated theory, we have performed a HF calculation of $\mu_N(B)$, choosing the states of the symmetric gauge as the complete basis set, with the Hilbert space truncated to the two spin-split states of the lowest orbital LL. We note that exact numerical calculations [7] for smaller N confirm the soundness of this truncation.

Because of the exchange term, the HF $\rho(r)$ differs from the SC result. In both models, the confinement energy favors a many-body state with the smallest area while the long range Coulomb repulsion prefers a state in which the electrons are the farthest apart. HF, however, adds an exchange energy which acts like a short range attractive interaction between parallel spins and favors occupation of adjacent orbitals (i.e., consecutive angular momentum index m) thus maximizing the electron density

[10]. For our small droplet size (small N and large $\hbar\omega_0$), the HF $\rho(r)$ has a two-tiered shape [10] with larger incompressible regions and smaller compressible regions (width $\sim\ell$) than the SC one. On the other hand, for large droplets (large N or small $\hbar\omega_0$), the HF $\rho(r)$ [10] resembles the domelike profile of the SC theory.

In Fig. 2(b), we plot χ_n extracted from $\mu_N(B)$ for the HF model with $N = 27$ electrons and $\hbar\omega_0 = 2.1$ meV. As with the SC model, these parameters are chosen to match the number of steps in the peak position and the experimental value of B_c, respectively. The HF value of $N = 27$ is different from that ($N = 42$) for the SC model, because of the difference in shape of $\rho(r)$. In the HF model, the GS below B_c is the state that minimizes S, i.e., $N_\uparrow = N_\downarrow + N(\text{mod}2)$ with $N = N_\uparrow + N_\downarrow$. Thus, the number of steps in $\mu_N(B)$ between B_c and $2B_c$ is equal to the integer part of $[N/2]$.

It is obvious from Fig. 2(b) that the HF calculation is in excellent quantitative agreement with the experiment [Fig. 2(a)], especially considering that there are no fitting parameters once N and $\hbar\omega_0$ are fixed. In particular, the HF model predicts correctly the apparent divergence of χ_n near B_c, in clear contrast with the SC model. A fit to the HF results with the empirical form $y(B)$ (see above) gives $\epsilon = -0.43 \pm 0.03$, the same as the experimental value within the errors.

A simple physical picture is helpful in understanding the divergence of χ_n near B_c. We approximate the total energy $\mathcal{E}$ of the droplet by $\mathcal{E} = \mathcal{E}_c + \mathcal{E}_Q$, where $\mathcal{E}_c$ is the confinement energy and $\mathcal{E}_Q$ is the Coulomb energy. We ignore the Zeeman energy $\mathcal{E}_Z$, because the bare g factor is small. This explains why the constant interaction model [6] that ignores $\mathcal{E}_Q$ and approximates instead $\mathcal{E}$ by $\mathcal{E}_c + \mathcal{E}_Z$ fails to describe the data even qualitatively [see Fig. 2(c)]. As mentioned above, the attractive exchange energy favors a compact occupation [10] so that for $B_c \leq B \ll 2B_c$ the HF GS has all the orbitals of angular momentum index $m = 0, \ldots, N_\downarrow - 1$ occupied for the $\downarrow$ spin and similarly for the $\uparrow$ spin. For this configuration $\mathcal{E}_c \propto \omega_0^2 S^2 \ell^2 + \text{const}$ for the parabolic confinement. The energy $\mathcal{E}_Q$ is expanded phenomenologically as $\mathcal{E}_Q = (-c_2 S^2 + c_4 S^4) e^2/\ell$ for $S < \sqrt{N}$ with $c_2 > N c_4$, two positive constants independent of B. Odd terms in S are absent due to the $N_\uparrow \leftrightarrow N_\downarrow$ symmetry. The magnetic fields at which spins flip can be obtained by requiring that $\mathcal{E}(S) = \mathcal{E}(S+1)$. This gives $B^{-3/2} - B_c^{-3/2} \propto S(S+1)$, so that for the first few spin flips $\chi \propto (B - B_c)^{-1/2} + \mathcal{O}(c_4/c_2)^2$, which is the form $y(B)$ with $\epsilon = -0.5$. Thus, the observed behavior at $B > B_c$ is caused by a gradual transition out of the $S = 0$ state. Although $\mathcal{E}_Z$ is negligible, the droplet still acquires a finite spin polarization $S \neq 0$ above B_c, because the cost in $\mathcal{E}_c$ for flipping a spin decreases with increasing B while the benefit in $\mathcal{E}_Q$ increases.

The apparent divergence of χ_n in Fig. 2(a) reflects the fact that $N_\uparrow \approx N_\downarrow$ just below B_c in our droplet. This is consistent with an independent experimental observation: A new step in $\mu_N(B)$ is added between B_c and $2B_c$ for every two electrons added [see Fig. 3(a)], implying that $N_\uparrow$ and $N_\downarrow$ are equally populated with increasing N.

Both the HF and SC calculations predict a spin polarized droplet ($S = N/2$) above $B_I = 3.2\ \text{T} = 1.9B_c$ for a wide range of N and $\hbar\omega_0$. Although we find a step at $2B_c$ in our measurement, there is also an additional step at $B_r = 3.8\ \text{T} = 2.2B_c$ (filled circle in Fig. 1) not predicted by the SC model. For all devices studied we find a step at $2B_c$, marking the complete depopulation of the higher energy spin state, and a step at larger field, in the spin polarized regime [14]. For one device, we have explored the phase diagram beyond $2.7B_c$ and have found evidence for other steps [15].

The step at B_r behaves in a way that is very different from that of those between B_c and $2B_c$. By examining successive peaks in G vs V_g (lower inset of Fig. 1), i.e., probing the droplet at successive N, we find that each step in μ_N shifts to higher B when another electron is added to the droplet. The part of the phase diagram we have measured is plotted in Fig. 3(a). We have averaged over four consecutive conductance peaks to measure the slopes of the phase boundaries $[B_n(N) - B_n(N-1)]^{-1}$, and these are plotted in Fig. 3(b) for each of the steps in Fig. 1. It is clear that the step at B_r has a larger slope than those at lower B.

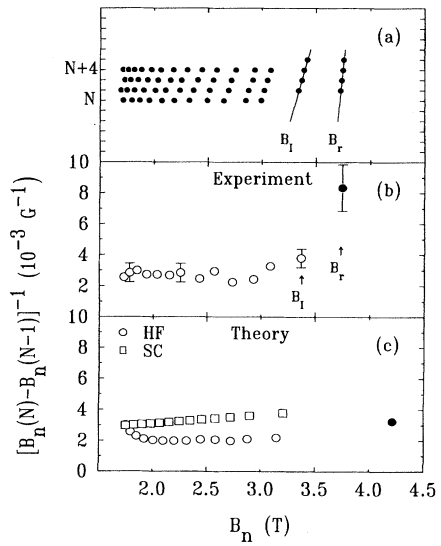

FIG. 3. (a) Experimental portion of the B-N phase diagram. The points are obtained by repeating the analysis described in the text on four consecutive conductance peaks (lower inset of Fig. 1). (b) The straight lines in (a) illustrate the determination of the slopes of the phase boundaries $[B_n(N) - B_n(N-1)]^{-1}$. The plotted value is the average over four consecutive peaks and the error bars are the standard deviations (c) HF and SC values of $[B_n(N) - B_n(N-1)]^{-1}$ measured from the simulated $\mu_N(B)$.

The temperature dependence (not shown) of the step at B_r is also peculiar [15]. The μ_N features between 1.7 and 3.4 T disappear by 500 mK as T is increased. This behavior is now well understood [1]. In clear contrast, the height of the step at $B_r = 3.8$ T does not change with temperature up to 800 mK, our measurement limit.

MacDonald, Yang, and Johnson [9] and Chamon and Wen [10] showed that there exists a region in the B-N phase diagram (sketched in the upper inset of Fig. 1) in which, for $N < N_c \sim 100$, the GS of the spin polarized droplet is the maximum density droplet (MDD). In the MDD state, all the single-particle eigenstates of angular momentum index $m = 0, 1, \ldots, N-1$ are occupied, for which $\rho(r)$ in the droplet is approximately constant at $(2\pi\ell^2)^{-1}$.

With increasing B, the radius of the MDD ($\sim\sqrt{2N}\ell$) decreases; the Coulomb interaction energy grows while the confinement energy diminishes eventually favoring a larger area droplet. HF [10] predicts that, at B_r, the edge undergoes a reconstruction and electrons form an annulus at a distance $\sim 2\ell$ away from the central droplet, causing an abrupt upward shift of μ_N at B_r of roughly the same height as the step at B_I [10]. In the HF calculation, B_r/B_I is weakly dependent on $\hbar\omega_0$, but it decreases with increasing N [9,10] for $N < N_c$.

In the HF model, the transition at B_r is only the first of a sequence of edge reconstructions [10] that tends, at high $B \gg B_r$, to make $\rho(r)$ resemble the hemispherical shape of the SC model. We believe that the measured transition at $B_r = 3.8$ T is the first edge reconstruction of the MDD. The HF calculation predicts that the first reconstruction occurs at 4.2 T for our droplet size, a value larger than the one observed experimentally. In this regard, it is important to bear in mind that although the HF energy of the MDD is exact because the MDD is an exact eigenstate of the many-body Hamiltonian [9], the HF energy of the reconstructed droplet is only variational. Therefore, the calculated value of B_r is an upper bound on the true transition field. Indeed, an exact calculation for small N [4,8] shows that the HF model overestimates B_r.

Returning to the slopes of the phase boundaries, one sees in Fig. 3(c) that $[B_n(N) - B_n(N-1)]^{-1}$ from HF ($\sim 2.2 \times 10^{-3}$ G^{-1}) agrees fairly well with experiment [$(3 \pm 1) \times 10^{-3}$ G^{-1}] between B_c and $2B_c$. However, at B_r, the HF value, 3.2×10^{-3} G^{-1}, appears to be smaller than the experimental value, $(8 \pm 1.5) \times 10^{-3}$ G^{-1}. The quantities $[B_n(N) - B_n(N-1)]^{-1}$ at B_I and B_r are the slopes of the phase boundaries in the B-N phase diagram between which the MDD is the GS. The fact that $[B_n(N) - B_n(N-1)]^{-1}$ is larger at B_r than at B_I suggests that the MDD does not exist above some N_c [9,10]. The experimental observation of both a larger value of $[B_n(N) - B_n(N-1)]^{-1}$ at B_r and a smaller value of B_r than the ones predicted by HF suggests that N_c is smaller than is predicted by HF.

The failure of HF to predict the size of the magnetic field window in which the MDD is the GS [Fig. 2(b)] and the dependence of B_r on N [Fig. 3(b)] may indicate that correlations are playing an important role in this transition. The downward step at about 3.5 T (Fig. 1) is also reminiscent of features predicted to result from correlations [4].

In conclusion, we have made a detailed study of the conductance peak positions in strong magnetic fields. We have focused on that part of the phase diagram in which only the lowest orbital LL with its two spin-split states is occupied. The experimental data suggest a divergent spin susceptibility at B_c in excellent quantitative agreement with HF. Below B_c, exchange favors a GS with minimum total spin and the observed behavior for $B_c < B < 2B_c$ is the result of a transition out of this nearly singlet state. Above $2B_c$, when the droplet is spin polarized, a new transition occurs at B_r which is only qualitatively described by HF.

We thank R. C. Ashoori, D. B. Chklovskii, D. Goldhaber-Gordon, K. A. Matveev, and N. S. Wingreen for many useful discussions. We also thank Nathan and Paul Belk for their help in the experiment. This work was supported by NSF Grant No. ECS 9203427 and by the U. S. Joint Services Electronics Program under Contract No. DAALL03-93-C-0001.

*Present address: Department of Physics, Weizmann Institute of Science, Rehovot 76100, Israel.

[1] P. L. McEuen *et al.*, Phys. Rev. Lett. **66**, 1926 (1991).
[2] R. C. Ashoori *et al.*, Phys. Rev. Lett. **71**, 613 (1993).
[3] M. A. Kastner, Phys. Today **46**, 24 (1993).
[4] S. R. Eric Yang, A. H. MacDonald, and M. D. Johnson, Phys. Rev. Lett. **71**, 3194 (1993).
[5] P. Hawrylak, Phys. Rev. Lett. **71**, 3347 (1993).
[6] P. L. McEuen *et al.*, Physica (Amsterdam) **189B**, 70 (1993).
[7] J. J. Palacios *et al.*, Phys. Rev. B **50**, 5760 (1994).
[8] D. Pfannkuche, R. R. Gerhardts, P. A. Maksym, and V. Gudmundsson, Physica (Amsterdam) **189B**, 6 (1993).
[9] A. H. MacDonald, S. R. Eric Yang, and M. D. Johnson, Aust. J. Phys. **46**, 345 (1993).
[10] C. de C. Chamon and X. G. Wen, Phys. Rev. B **49**, 8227 (1994).
[11] U. Meirav, M. A. Kastner, and S. J. Wind, Phys. Rev. Lett. **65**, 771 (1990).
[12] A. Kumar, S. E. Laux, and F. Stern, Phys. Rev. B **42**, 5166 (1990).
[13] C. W. J. Beenakker, Phys. Rev. B **44**, 1646 (1991).
[14] We point out that while the results reported here are completely reversible and continuous [16], we have, from time to time, observed hysteresis behavior in strong magnetic fields.
[15] O. Klein *et al.* (unpublished).
[16] N. C. van der Vaart *et al.*, Phys. Rev. Lett. **73**, 320 (1994).